

Document downloaded from:

<http://hdl.handle.net/10251/150630>

This paper must be cited as:

Bernat-Quesada, F.; Espinosa-López, J.C.; Barbera, V.; Alvaro Rodríguez, M.M.; Galimberti, M.; Navalón Oltra, S.; García Gómez, H. (2019). Catalytic Ozonation Using Edge-Hydroxylated Graphite-Based Materials. *ACS Sustainable Chemistry & Engineering*. 7(20):17443-17452. <https://doi.org/10.1021/acssuschemeng.9b04646>



The final publication is available at

<https://doi.org/10.1021/acssuschemeng.9b04646>

Copyright American Chemical Society

Additional Information

"This document is the Accepted Manuscript version of a Published Work that appeared in final form in *ACS Sustainable Chemistry & Engineering*, copyright © American Chemical Society after peer review and technical editing by the publisher. To access the final edited and published work see <https://doi.org/10.1021/acssuschemeng.9b04646>"

Catalytic ozonation using edge-hydroxylated graphite-based materials

Francisco Bernat-Quesada,^{1,†} Juan C. Espinosa,^{1,†} Vincenzina Barbera,^{2,*} Mercedes
Álvaro,¹ Maurizio Galimberti,^{2,*} Sergio Navalón^{1,*} Hermenegildo García^{1,3,4*}

¹ Departamento de Química, Universitat Politècnica de València, C/Camino de Vera,
s/n, 46022 Valencia, Spain

² Politecnico di Milano, Department of Chemistry, Materials and Chemical Engineering
'G. Natta', Via Mancinelli 7, 20131 Milano, Italy

³ Instituto Universitario de Tecnología Química, CSIC-UPV, Universitat Politècnica de
Valencia, Av. de los Naranjos, Valencia 46022, Spain

⁴ Center of Excellence for Advanced Materials Research, King Abdulaziz University,
Jeddah, Saudi Arabia

† Both are considered as first authors

Emails:

vincenzina.barbera@polimi.it

maurizio.galimberti@polimi.it

sernaol@doctor.upv.es

hgarcia@qim.upv.es

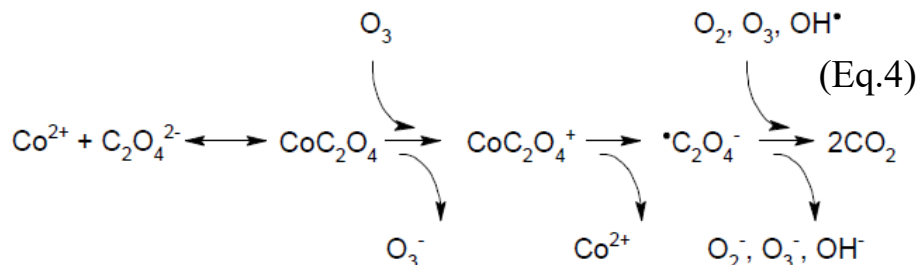
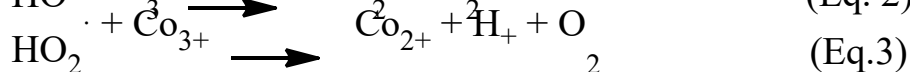
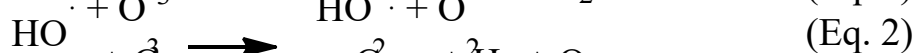
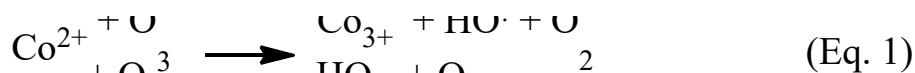
ABSTRACT

This work reports the catalytic ozonation activity of high surface area graphite materials selectively functionalized at the edges with hydroxyl groups. The graphite-based catalyst shows higher activity than the parent graphite, commercial activated carbon, commercial multiwall carbon nanotubes, commercial diamond nanoparticles, graphene oxide or reduced graphene oxide. Importantly, the catalytic activity of the graphite-based material is also higher than those of benchmark ozonation catalysts such as Co_3O_4 or Fe_2O_3 . The graphite catalyst was reused up to ten times with only a minor decrease in the catalytic activity. Catalytic activation of O_3 leads to the generation of hydroperoxide radicals and $^1\text{O}_2$. These results have been interpreted as derived from the combination of suitable work function and the presence of phenolic/semiquinone-like redox pairs as well as high dispersability in water due to the presence of $-\text{OH}$ group. This work highlights the possibility of engineering active and stable carbocatalysts for reactions typically promoted by transition metals.

KEYWORDS: metal-free catalysts; carbocatalysis; graphite as catalyst; ozone activation; oxalic acid degradation

INTRODUCTION

Most of industrial chemical processes employ transition metals as catalysts.¹⁻⁵ In the field of environmental applications, advanced oxidations processes (AOPs) employing catalysts are among the preferred technologies for water pollution remediation.⁶⁻¹¹ The most efficient AOPs are based on the use of strong oxidants such as ozone, hydrogen peroxide or peroxymonosulfate/persulfate and transition metal ions as homogeneous catalysts.^{6, 9, 12-14} Unfortunately, homogeneous catalysis for water remediation has the drawback of the need to remove, in some cases at trace level, the metals employed as catalysts.¹⁵ In this regard, heterogeneous catalysis for AOP may overcome some of the important limitations of homogeneous catalysis.¹⁵⁻²⁰ Heterogeneous catalytic ozonation is an AOP that can be potentially implemented at industrial scale.^{12, 21} Many potable or wastewater treatment plants have already installed in their facilities ozone generators, being on this way easier to implement a catalytic process. Regardless of its relatively high oxidation potential, E^0 2.07 V, O_3 in the absence of catalysts is not reactive enough to degrade some toxic and recalcitrant pollutants, such as deactivated aromatic compounds and electron-poor aliphatic contaminants.¹² For this reason, the objective of catalytic ozonation is to generate from O_3 other reactive oxygen species (ROS), such as hydroxyl or hydroperoxyl radicals (Equations 1-4) able to unselectively degrade a wide range of recalcitrant pollutants such as oxalic acid.^{12, 21-23} As in the case of homogeneous catalysis, the most efficient heterogeneous catalysts to promote ozonation by generating ROS are, however, transition metals such as cobalt, manganese, iron, cerium, titanium, among others.^{21, 24}



In view of these precedents it would be convenient to develop additional sustainable and efficient heterogeneous catalysts not based on transition metals for ozonation.²⁵⁻²⁸ In this context, several groups have employed and/or modified activated carbons²⁹⁻³⁷ and, to a lesser extent, other carbonaceous materials such as activated carbon fibers³⁸ or multiwalled carbon nanotubes (MWCNTs)^{31, 39} as carbocatalysts for ozone activation. The discovery of graphene (G) in 2004 extended further the interest for carbon-based materials as catalysts.^{40, 41} Recently, reduced graphene oxide (rGO) has been reported as a heterogeneous carbocatalyst to promote the catalytic ozonation.⁴² It was observed, however, that rGO becomes deactivated to a large extent even after one use. In addition, rGO preparation was based on the Hummers method that generates a large amount of wastes.⁴³

Herein, the preparation of a highly active, stable and economically attractive graphite-based catalyst, obtained from commercially available high surface area graphite (HSAG) simply modified at the edges by hydroxyl groups using KOH as reagent (HSAG-OH) is reported. It was observed that the ozonation activity of HSAG-OH is higher than those of several other carbon-based materials, such as graphite (G), commercial HSAG, carbon nanotubes (CNTs), activated carbon, nanometric diamond,

graphene oxide, rGO and even higher than that achieved using benchmark metal oxides such as Co_3O_4 , CeO_2 , Al_2O_3 or CuO . HSAG-OH was reused efficiently ten times. Importantly, a reductive thermal treatment of the ten times-used catalyst allows the recovery of its excellent catalytic activity for ozone activation to hydroperoxyl radicals. Based on the comparison of the catalytic activity of HSAG-OH with that of several other carbonaceous catalysts it will be concluded that the high activity of the HSAG-OH derives from the integrity of sp^2 graphene layers in a multilayer configuration together with its excellent dispersibility of the HSAG-OH particles in aqueous medium due to the presence of peripheral OH groups.

EXPERIMENTAL SECTION

Materials

Graphite (CAS 7782-42-5), diamond nanoparticles (ref: 636 444, $\geq 97\%$), activated carbon (AC, Norit SX Ultra, ref 53663), Al_2O_3 , CeO_2 , Co_3O_4 , CuO , dimethylsulfoxide (DMSO, $>99.5\%$), 5,5-dimethyl-1-pyrroline N-oxide (DMPO), 2,2,6,6-tetramethylpiperidine (TEMP) were supplied by Sigma-Aldrich. MWCNTs were supplied by Nanostructured & Amorphous Materials. HSAG was Synthetic Graphite 8427[®] supplied by Asbury Graphite Mills Inc. Characterization of HSAG has been reported by some of us in previous studies.⁴⁴⁻⁴⁷ Other reagents employed were analytical or HPLC grade and they were also provided by Sigma-Aldrich.

HSAG oxidation by nitric acid. As previously reported for analogous carbonaceous materials, commercial HSAG (1 g) was dispersed in $\text{HNO}_3(\text{c})$ (25 mL) in a round-bottom flask, and the mixture heated under stirring at $83\text{ }^\circ\text{C}$ for 20 h.⁴⁸ After cooling the reaction system, the suspension was centrifuged at 12,000 rpm for 20 min and washed repeatedly with Milli-Q water until the pH value of the washing liquids was neutral.

Finally, the solid sample was recovered by filtration and dried at 100 °C for 12 h. This sample was labelled as HSAG-HNO₃.

HSAG hydroxylation by KOH. As previously reported^{44, 45} HSAG and KOH were reacted in a planetary ball mill S100 from Retsch, with 0.3 L grinding jar moving on a horizontal plane. The jar was loaded with 6 ceramic balls having a diameter of 20 mm. HSAG (1 g), KOH powder (20 g) and H₂O (6.5 mL) were put into the jar that was rotated at 300 rpm, at room temperature, for 10 h. After this time, the mixture was placed in a Büchner funnel with a sintered glass disc and repeatedly washed with distilled water (6 × 100 mL) under vacuum. Finally, the obtained solid was put in an oven at 60 °C to remove excess water. This sample was labelled as HSAG-OH. Recently, possibility to perform edge-oxidation of graphites by hydrogen peroxide oxidation has been recently reported.⁴⁹

HSAG-OH functionalization by means of the Reimer-Tiemann/Cannizzaro domino. As previously reported, in a round bottomed flask equipped with magnetic stirrer and condenser, KOH powder (3.12 g, 55 mmol), CHCl₃ (1.12 mL, 14 mmol) and H₂O (0.5 mL) were added in sequence. HSAG-OH (0.500 g) was added to such mixture after few seconds.⁴⁴ The mixture was stirred at room temperature, for 12 h. After this time, the solvent was removed at reduced pressure. The resulting solid was ground in fine grains in a mortar with a pestle, transferred into a Falcon™ tube (15 mL) and water (10 mL) was added. The suspension was sonicated for 10 min and centrifuged at 4000 rpm for 10 min (3 times). This sample was labeled as HSAG-OH-COOH.

Reactivation of the HSAG-OH sample after 6 uses.

Method A: Heating treatment. 0.1 g of 6 times used HSAG-OH sample and CH₂Cl₂ (25 mL) were put in a 50 mL round bottomed flask equipped with magnetic stirrer. The resulting suspension was stirred at room temperature for 12 h. After this time the

mixture was filtered and the powder was put in a 5 mL glass vial and heated at 200 °C for 12 h under nitrogen atmosphere.

Method B: Reduction by hydrazine. 0.1 g of 6 times used HSAG-OH sample were put in a 25 mL round bottomed flask equipped with magnetic stirrer. To this suspension, hydrazine monohydrate (1 μ for 1 mg of HSAG-OH) was added. The suspension was stirred at 80 °C for 12 h. After this time the mixture was filtered and the powder was dried.

Pyrolyzed nanometric diamond. Commercial diamond nanoparticles (NPs) (200 mg) were placed in a tubular oven under Ar atmosphere and heated up to 900 °C at 5 °C/min for 1 h. After cooling the system at room temperature, the samples were washed with ethanol and water and finally dried at 100 °C for 12 h.⁵⁰

Characterization

Combustion elemental analyses were performed using a CHNOS analyzer (Perkin Elmer). Raman spectra were collected at room temperature upon 514 nm laser excitation using a Renishaw In Via Raman spectrophotometer equipped with a CCD detector. Temperature-programmed desorption (TPD) coupled to a mass-spectrometer (TPD-MS) analyses of the carbonaceous samples were collected in a Micrometer II 2920 station connected to a quadrupolar mass spectrometer. X-ray photoelectron spectroscopy (XPS) measurements were performed with a SPECS spectrometer with an MCD-9 detector using a monochromatic Al ($K\alpha= 1486.6$ eV) X-ray source. The C1s peak at 284.4 eV was employed as reference. Transmission electron microscopy (TEM) images of nanometric diamond samples were acquired using a JEOL JEM-2100F instrument operating at 200 kW.

Catalytic reactions

Catalytic ozonations. Ozone was generated from dried-air using a commercially available corona discharge ozone generator. The generated ozone (140 mg/h) was introduced at 570 mL/min through a gas diffuser into the bottom of a 300 mL glass reactor. Typically, the reactor contained 250 mL of Milli-Q water with or without oxalic acid (50 mg L⁻¹) as model organic pollutant together with the dispersed catalyst (100 mg L⁻¹). The course of the reaction was followed by analyzing immediately after being taken reaction aliquots previously filtered through a Nylon filter (0.2 μm) to remove the catalyst.

Selective quenching experiments and EPR measurements. These experiments were performed similarly as described for oxalic acid degradation at pH 3, but: i) for selective hydroxyl quenching experiments, dimethylsulfoxide or *tert*-butanol (20 mol % with respect to oxalic acid) were also present; ii) for EPR experiments oxalic acid was replaced DMPO or TEMP as ROS trapping agent at 1 g L⁻¹. EPR measurements were carried out in a Bruker EMX spectrometer (9.803 GHz, sweep width 3489.9 G, time constant 40.95 ms, modulation frequency 100 kHz, modulation width 1 G, microwave power 19.92 mW) at pH 3 and 20 °C and 20 min of reaction.

Ozone measurements. Ozone calibrations were carried out by iodometry. To determine ozone self-decomposition or decomposition in the presence of carbonaceous solids (50 mg L⁻¹) in water, the pH value of the aqueous solution or suspension was first adjusted using HCl or NaOH aqueous solutions, then the absorbance of aliquots was measured in a UV-Vis spectrometer (Jasco instruments) from 200 to 400 nm. It should be noted that O₃ exhibits a maximum absorption wavelength at 260 nm with an extinction coefficient of 3000 M⁻¹ cm⁻¹.⁵¹

Oxalic acid analysis. Oxalic acid concentration was determined by analyzing reaction aliquots by ion-chromatography using a conductivity detector. The stationary phase was a polyvinyl alcohol with quaternary ammonium groups column, while the mobile phase was a basic aqueous solution (3.2 mM Na₂CO₃ / 1.0 mM NaHCO₃ mM).

Total organic carbon (TOC). TOC of aqueous oxalic acid solutions was analyzed using a High TOC Elementar II analyzer.

Boehm titration. It was performed to quantitatively determine the content of oxygenated surface groups. In a typical experiment, 0.05 g of the carbon allotrope were dispersed in 50 mL of a 0.05 M NaOH solution and water was removed (see in the following). After stirring at room temperature for 24 h, the mixture was filtered. Removal from the solution of the solid carbon allotrope is essential to avoid the reaction of deprotonated groups on carbon allotrope surface with HCl. A portion of the solution (10 mL) was mixed with a water solution of HCl (0.05 N, 20 mL). CO₂ was removed from solution immediately before the titration. The obtained mixture was titrated using a 0.05 M solution of NaOH.

CO₂ removal with N₂. The samples were poured in 40 mL glass vials equipped with a glass septum lids. N₂ was bubbled into the vial through a needle submerged in the solution. Bubbling rate was less than 1 mL/min. The time of degasification was 24 h. After degasification, the samples were transferred to a beaker that had been purged with the inert gas and covered with Parafilm[®], to prevent absorption of atmospheric CO₂.

UV-vis titration of O₃. A Hewlett Packard 8452A Diode Array Spectrophotometer was used to perform the optical absorption measurements. The dispersions in where the concentration of O₃ wanted to be determined (circa 3 mL) were placed with a Pasteur pipette in 1 cm optical path quartz cuvette. The UV-visible spectrum reported the absorption as a function of the wavelength of the radiation between 200 and 750 nm.

RESULTS AND DISCUSSION

Catalyst characterization

Table 1 lists the carbon materials employed as catalysts in the present work, their precursors and the preparation methods. The preparation and characterization of some of materials have been already reported and references are provided to the articles where these materials were originally disclosed. The synthesis of two other carbon materials, namely HSAD-HNO₃ and PD in Table 1, has been performed for the first time for this work. Among the most relevant characterization data, XPS provides information of the elements present on the catalyst surface, their relative abundance and their distribution among the different families. To illustrate the relevant data obtained by XPS, Figure 1 shows C1s and O1s peaks recorded for HSAG-OH that, as it will be commented below, is the most active ozonation catalyst. As it can be seen in this Figure, both C and O elements are present on the surface with an atomic proportion of 91.3 and 8.7 %, respectively, and their high resolution experimental peak can be fitted to four and three components for the C and O, respectively. We will come back later to this point when commenting the active sites on edge functionalized graphite and the deactivation mechanism.

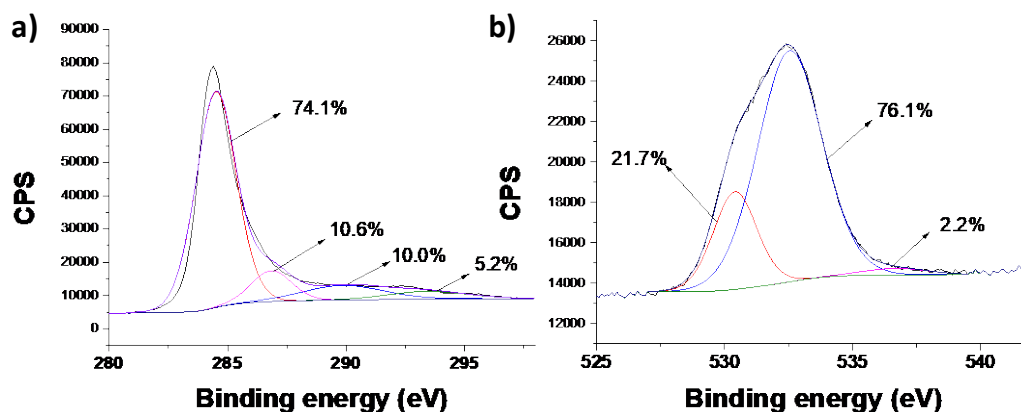


Figure 1. XPS C1s (a) and O1s (b) peaks of fresh HSAG-OH. The figure shows also the best deconvolution of the experimental peaks to individual components and their corresponding percentages.

Among the samples tested a high-surface area graphite modified with oxygen-functional groups both at edges and on the basal planes was prepared via HNO₃ oxidation treatment (HSAG-HNO₃), similarly to other reported carbonaceous materials.⁴⁸ The oxidation of HSAG material by HNO₃ was confirmed by combustion elemental analysis that provides an estimation that the oxygen content of HSAG-HNO₃ is about 12 wt%. It should be commented that the oxygen content in the commercial HSAG is negligible. XPS C1s and O1s peaks of the HSGA-HNO₃ also confirm the presence on the HSAG surface of oxygen-functional groups having single, double and three C-O bonds such as alcohols, carbonyl and carboxylic derivatives (Figure S1). These oxygen functional groups were also evidenced by FT-IR spectroscopy. Vibration bands at 3300, 1710 and 1200 cm⁻¹ are characteristic of O-H, C=O and C-O bonds, present in alcohols, carbonylic and carboxylic functional groups, respectively.

Pyrolyzed diamond NPs (PD) was prepared by pyrolysis of commercial nanodiamonds (D) at 900 °C as previously reported.⁵⁰ Raman spectroscopy of PD clearly shows the formation of defective sp² network characterized by the observation of the D, G and 2D bands that are absent in the parent D sample (Figure S2a). TPD characterization of PD also confirms the removal of surface functional groups present in the commercial D sample (Figure S2b). In addition, solid state ¹³C-NMR spectrum of PD shows the presence of carbon atoms with sp² and sp³ hybridization (Figure S3). Previous studies by our group have reported the absence of sp² carbon on commercial D NPs.⁵² The formation of graphene layers on the surface of D upon pyrolysis at 900 °C agrees with a recent report describing also the formation of a few outer graphene layers

in a core/shell configuration upon pyrolysis of diamond NPs (Figure S4). In fact, HRTEM of PD further confirms the formation of graphene layers with an interplanar distance of 3.38 Å while the sp^3 interplanar distance in D NPs is around 2.02 Å. These values measured in the present study are close to the reported 3.56 and 2.06 Å interplanar distances for graphite and D, respectively (Figure S5).⁵³.

Table 1. List of catalysts employed in the present work.

Entry	Name	Abbreviation	Precursor/Preparation method	Ref.
1	Graphite	G	Commercial	
2	High-surface area graphite	HSAG	Commercial	
3	HSAG functionalized with hydroxyl groups in the edges	HSAG-OH	HSAG/KOH	44, 46
4	HSAG functionalized with OH and COOH groups in the edges	HSAG-OH-COOH	HSAG/ KOH	44
5	HSAG functionalized with oxygen-functional groups in both edges and basal plane	HSAG-HNO ₃	HSAG/HNO ₃	This work
6	Graphene oxide	GO	Graphite/Hummers method	54
7	Reduced graphene oxide	rGO	GO/thermal reduction at 200 °C	54

8	Multiwall carbon nanotubes	MWCNTs	Commercial	-
9	Diamond nanoparticles	D	Commercial	-
10	Hydroxylated diamond NPs	D-OH	Chemical treatment+hydrogen annealing of D NPs	⁵⁵
11	Pyrolyzed diamond NPs	PD	D NPs/pyrolysis at 900 °C for 2 h	This work
12	Activated carbon	AC	Commercial	-

Catalytic activity

Comparison of catalytic efficiency of various carbon materials. In the first stage of the work the efficiency of different carbonaceous materials as catalysts for the ozonation of organic pollutants in water was compared. Oxalic acid was selected as probe molecule to determine the efficiency of the catalytic ozonation (Figure 2a).^{14, 23} Graphs of Figure 2 show the dependence on time of the concentration of oxalic acid upon reacting with ozone, both in presence of different carbocatalysts (a) as well as in the presence of transition metal catalysts (b) and at different pH with HSAG-OH as the catalyst (c).

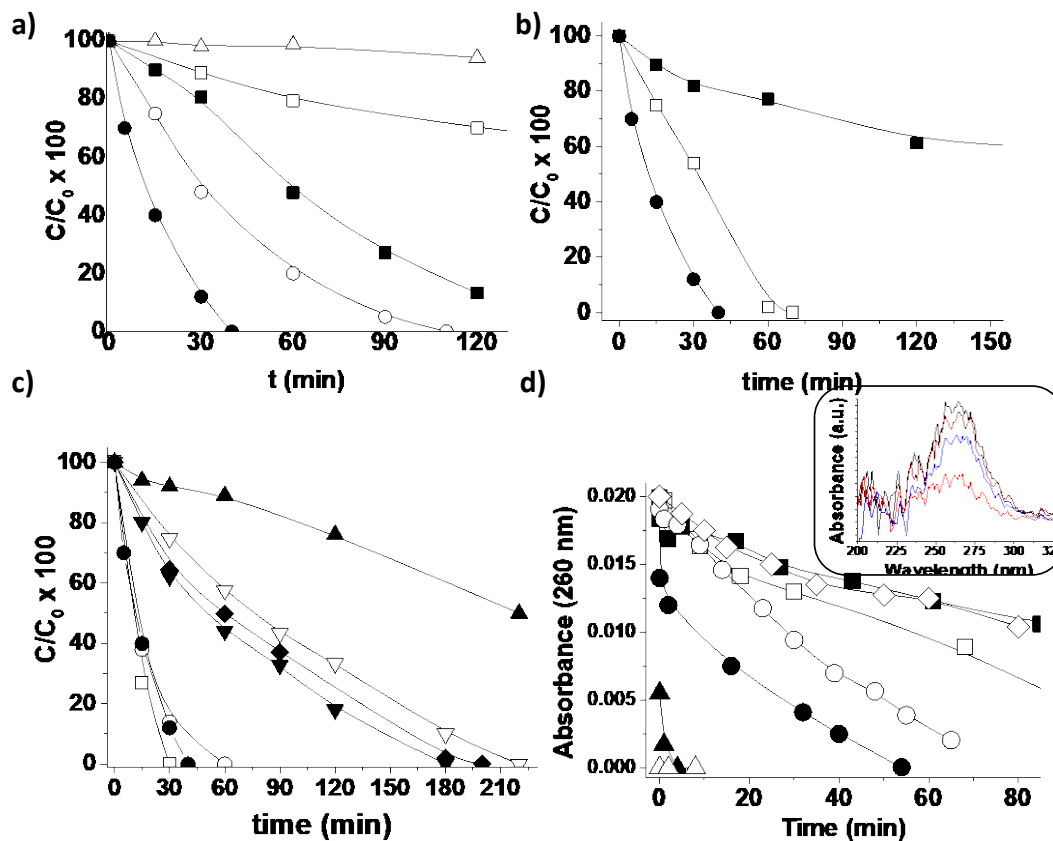


Figure 2. Decomposition of oxalic acid by ozone. a) Relative oxalic acid concentration vs time at pH 3 without catalyst (Δ) or in presence of HSAG-OH (\bullet), HSAG (\circ), rGO (\blacksquare), GO (\square) as catalysts; b) Relative oxalic acid concentration vs time at pH 3 in presence of: HSAG-OH (\bullet), Co_3O_4 (\square) or Fe_2O_3 (\blacksquare) as catalysts. c) Relative oxalic acid concentration vs time in presence of HSAG-OH as catalyst, at: pH 2 (\square), pH 3 (\bullet), pH 4 (\circ), pH 5 (\blacktriangledown), pH 7 (∇), pH 9 (\blacklozenge) and pH 12 (\blacktriangle). d) Ozone stability in water in the absence of catalyst as function of the pH. Legend: pH 2 (\blacksquare), pH 3 (\diamond), pH 5 (\square), pH 7 (\circ), pH 9 (\bullet), pH 10 (\blacktriangle) and pH 12 (\triangle). Reaction conditions: catalyst (50 mg L^{-1}), oxalic acid (50 mg L^{-1}), O_3 (140 mg/h), pH as indicated, $20 \text{ }^\circ\text{C}$. O_3 to oxalic acid molar ratio 5.3. The inset shows the UV absorption band corresponding to O_3 at 260 nm

As previously reported,¹⁴ blank control experiments in the absence of catalyst reveal that ozone cannot degrade oxalic acid at pH 3 and 20 °C.²³ In general, oxalic acid adsorption on the different carbonaceous materials at pH 3 and 20 °C is lower than 2 wt%. Importantly, under these experimental conditions, oxalic acid can be degraded by catalytic ozonation using different carbonaceous materials: HSAG-OH (•), HSAG (○), GO (□), rGO (■). The most active carbocatalyst is that based on commercial HSAG functionalized with hydroxyl groups in the edges (HSAG-OH), followed by the commercially available parent HSAG. Both HSAG-based catalysts are more active than previously reported rGO obtained from a Hummers method followed by thermal reduction at 200 °C.⁴² In agreement with previous reports, the catalytic activity of GO was lower than that of rGO.⁵⁶ Considering the structure of the various catalysts these results reinforce the importance of an appropriate content of oxygen functional groups together with sp² carbon domains as active sites of ozonation in carbocatalysts. This proposal agrees also with other studies that have reported higher carbocatalytic activity of rGO with respect to GO as catalysts of oxidations using H₂O₂ or PMS as reagents.²⁷ Importantly, the carbocatalytic activity of HSAG-OH resulted to be higher than that of benchmark commercial inorganic catalysts as Co₃O₄ or Fe₂O₃ (Figure 2b).^{12, 21}

One of the most important parameters that influences the efficiency of catalytic AOPs is the pH value of the water to be treated.^{9, 16, 57} Figure 2c shows that HSAG-OH is an efficient ozonation carbocatalyst in a broad pH window, from 2 to 9 units, with optimum values around 4. The broad range of pH for carbocatalytic ozonation, using HSAG-OH, makes the application of this carbocatalyst really feasible for wastewaters whose pH is either acidic or slightly basic. It should be noted that blank control experiments, performed in the absence of catalysts, do not significantly degrade oxalic

acid (< 8 % conversion), in the range of the adopted pH values, except at pH \geq 12, where slightly higher oxalic acid degradation was observed (~20 % at 240 min).

In order to determine the ozone stability in water at different pH values in the absence of catalyst, a series of control experiments were carried out (Figure 2d). In agreement with previous reports, O₃ stability decreases as the pH of the aqueous medium increases.¹² In fact, at pH values higher than 10, O₃ is almost instantaneously decomposed under the present reaction conditions. It is well-established that O₃ decomposes spontaneously to reactive oxygen species such as hydroperoxyl radicals at basic pH values.¹²

Ozone dose consumption is a decisive factor for the development of AOP with real potential applications.²² In the present work, additional experiments have been conducted for the optimization of the ozone dose. It was observed that, by using HSAG-OH as catalyst, complete oxalic acid degradation at both pH 3 and 5 takes place when using 2.7 equivalents of O₃ (Figure S6)²². This value represents a moderate excess respect to the stoichiometric amount necessary to convert oxalic acid into CO₂.

Stability of carbocatalysts. One of the basic requirements of any catalyst is its stability under reaction conditions. This aspect was in particular investigated for HSAG-OH and rGO as the catalysts. Results of reusability test are shown in Figure 3. HSAG-OH was reused up to ten times with only a slight decrease in catalytic activity and full oxalic acid degradation was achieved, at longer reaction times (Figure 3a). These results are definitely better than those collected with rGO prepared by the Hummers method, which rapidly deactivates after one use (Figure 3b). Based on a previous work, thermal treatment of the rGO sample in a muffle at 300 °C allows restoring its catalytic activity.⁴²

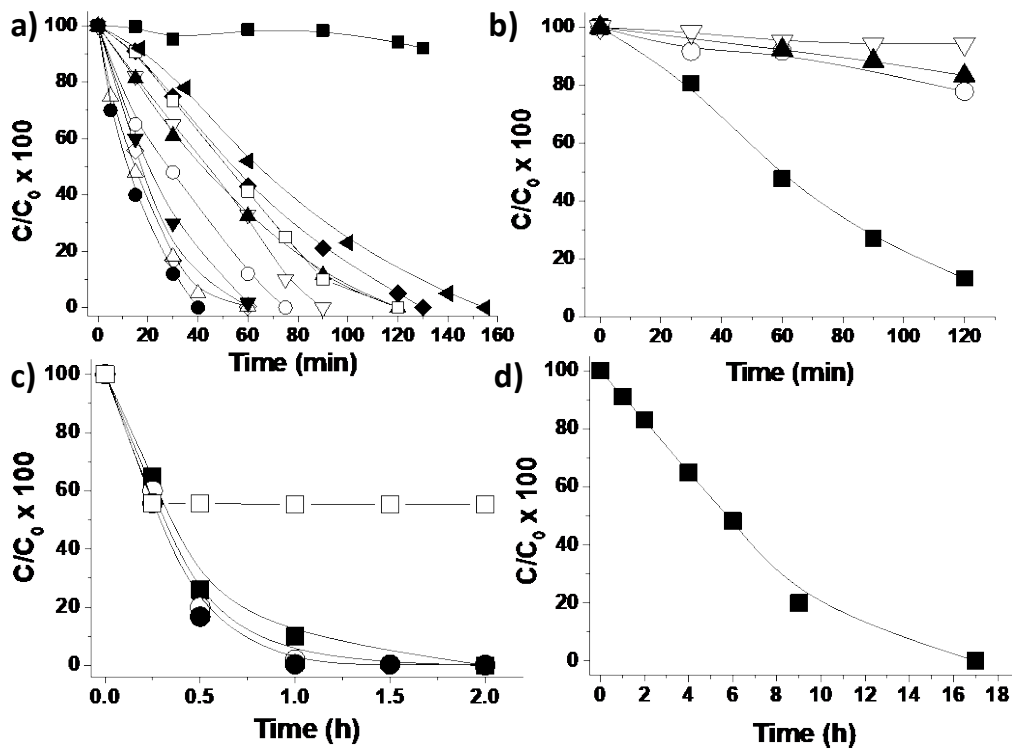


Figure 3. Reaction of oxalic acid with ozone. All the graphs show the relative oxalic acid concentration vs time. (a) Catalyst: HSAG-OH: a) 1st use (●), 2nd use (△), 3rd use (◇), 4th use (▼), 5th use (○), 6th use (▽), 7th use (▲), 8th (□), 9th use (◆), 10th (◄) and reaction in the absence of catalyst (■). (b) Catalyst: rGO: 1st use (■), 2nd use (○), 3rd use (▽) and 4th use (▲). (c) Catalyst: HSAG-OH (●), HSAG-OH removed at 44 % oxalic degradation (□), HSAG-OH after 6 uses and then pyrolyzed under Ar atmosphere (■) HSAG-OH after 6 uses and then reduced with hydrazine (○). (d) Productivity test using a large excess of oxalic acid using HSAG-OH as catalyst. Reaction conditions: Catalyst (50 mg L⁻¹), oxalic acid (50 mg L⁻¹), O₃ (140 mg/h), pH 3, room temperature. O₃ to oxalic acid molar ratio 5.3. Reaction conditions of productivity test: Catalyst (50 mg L⁻¹), oxalic acid (1 g L⁻¹), O₃ (140 mg/h), pH 3, room temperature. O₃ to oxalic acid molar ratio 5.3

XPS of the six-times used HSAG-OH (Figure 4 and Figure S7) reveals the partial oxidation of the carbon material during the carbocatalytic reaction. According to deconvolution of the XPS O1s peak the deactivated HSAG-OH sample exhibits an increase of the quinone-like oxygens (binding energy 532.5 eV) accompanied by a concomitant decrease of the phenolic-like oxygen (binding energy 530 eV) (Figure 4c vs 4d). Therefore, comparison of the XPS O1s of the fresh and deactivated material suggests the role as active sites of phenolic/quinone-like moieties as redox pair promoting the O₃ activation. Similar proposal of phenolic/quinone-like redox pairs as active sites was postulated by Su and co-workers for the carbocatalytic oxidative dehydrogenation of ethylbenzene,^{58, 59} and is in line with the ability hydroquinones to promote Fenton-like chemistry as organocatalysts.^{54, 60} Importantly, the catalytic activity of the ten-times used HSAG-OH can be restored to the value of the fresh sample by performing a reduction process either with hydrazine as reducing agent or by thermal reduction at 300 °C (Figure 3c and Figure 4e-f). XPS of the ten-times used HSAG sample treated by thermal treatment or hydrazine confirms the success of the reduction process restoring the fresh HSAG-OH material by observing the coincidence of the C1s and O1s peaks of the treated samples with those of the fresh HSAG that are different from the ten-times used material (Figure 4 and S8).

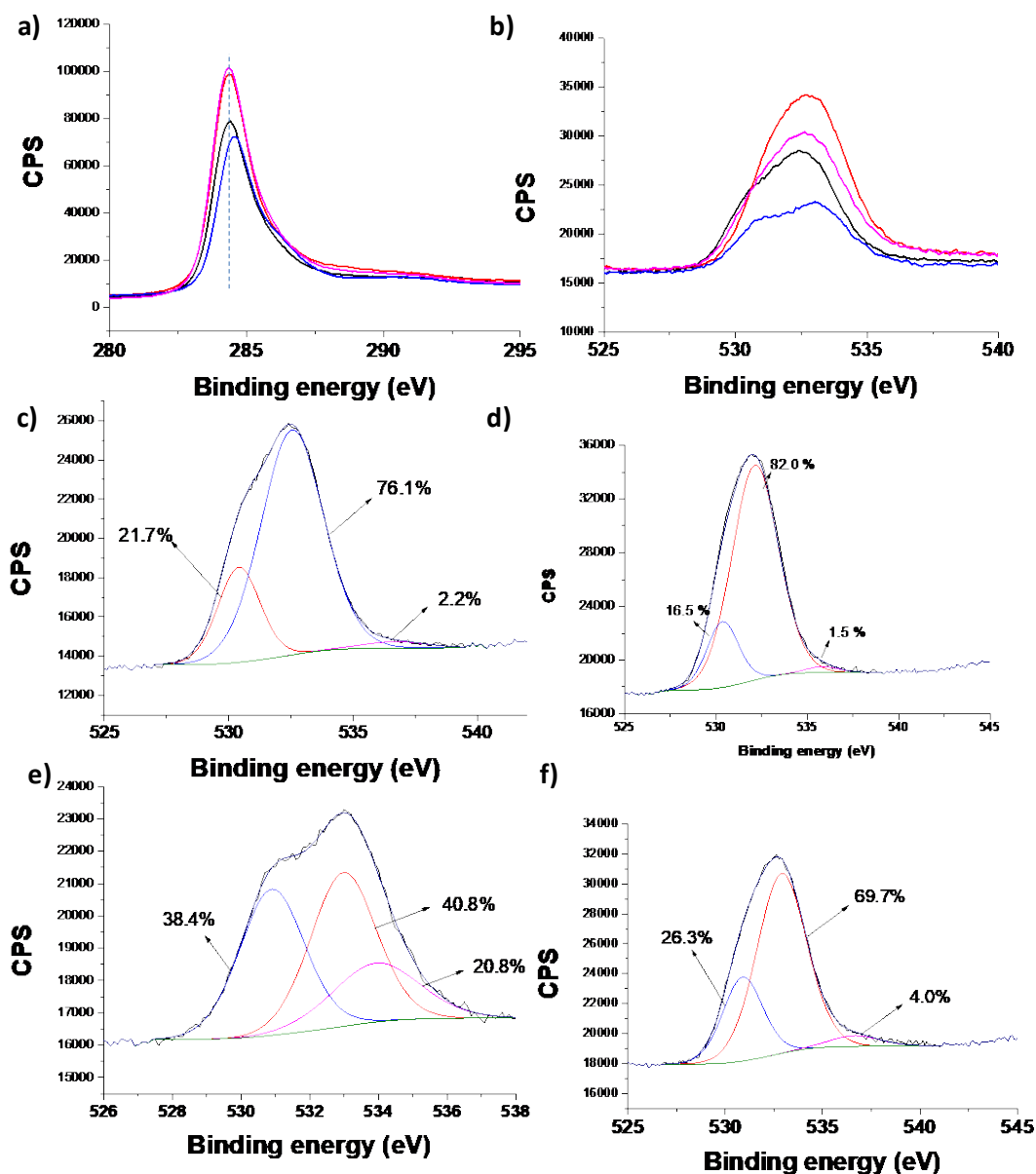


Figure 4. XPS C1s (a) and O1s peaks (b) for the fresh HSAG-OH (black line), six times used HSAG-OH in oxalic acid ozonation (red line), six times used HSAG-OH followed by thermal reduction at 300 °C (blue line) and six times used HSAG-OH regenerated by chemical reduction with hydrazine (pink line). XPS O1s for fresh HSAG-OH (c), six times used HSAG-OH in oxalic acid ozonation (d), six times used HSAG-OH followed by thermal reduction at 300 °C (e) and six times used HSAG-OH regenerated by chemical reduction with hydrazine (f) have been fitted to the best deconvolution of the experimental peaks into individual components.

The heterogeneity of the reaction was assessed by observing that the reaction stops if the catalyst is removed from the reaction and, then, ozonation is continued under the same reaction conditions (Figure 3c, □).

The excellent activity and stability of the HSAG-OH as carbocatalyst was further established by performing a productivity test, observing that a small amount of carbocatalyst (50 mg L^{-1}) is able to degrade up to 1 g L^{-1} of oxalic acid (Figure 3d).

Insights into the catalytic activity of HSAG-OH. In order to get some insights into the origin of the catalytic activity of HSAG-OH, several commercially available carbon materials with or without further modification were also used as catalyst to correlate structure and activity. The temporal profiles of the oxalic acid decomposition by ozone in the presence of the different carbocatalysts are presented in Figure 5.

A first working hypothesis to explain the higher activity of HSAG-OH with respect to HSAG was based on the presence of phenolic functional groups at the graphene edges, which leads to a better water dispersability, an increase in the work function of the graphene sheets and the presence of hydroquinone/quinone-like groups as redox centers.

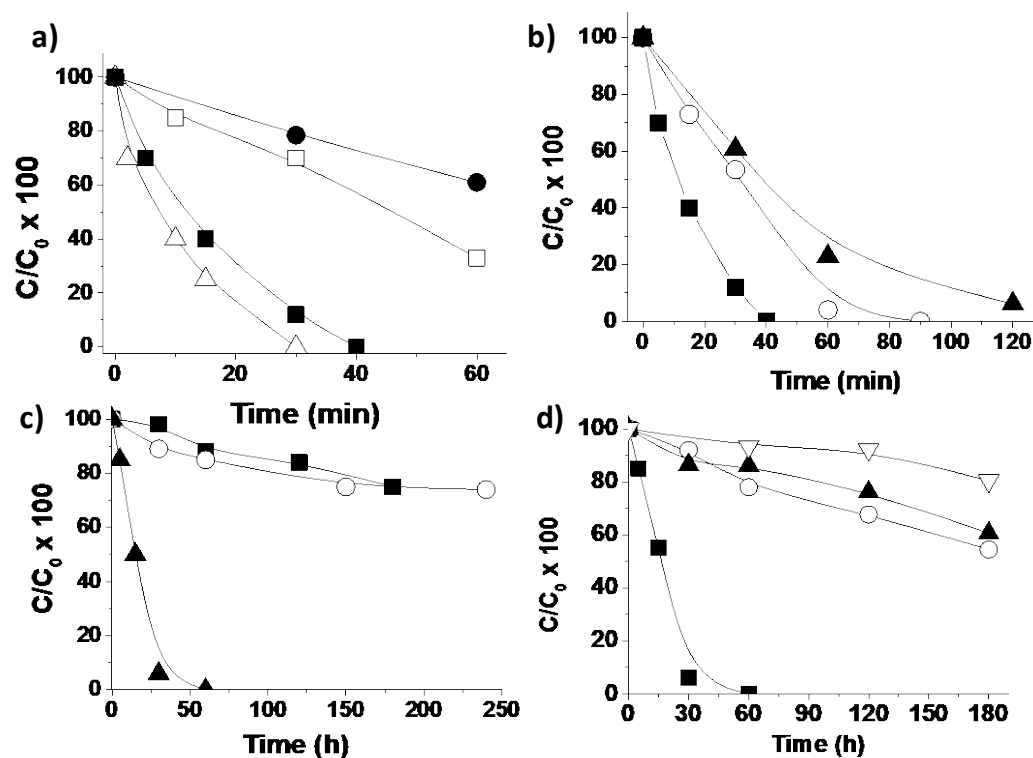


Figure 5. Temporal evolution of oxalic acid concentration upon ozonation in the presence of various catalysts. Catalysts: a) HSAG-OH-COOH (Δ), HSAG-OH (\blacksquare), HSAG-HNO₃ (\square), graphite (\bullet); b) HSAG-OH (\blacksquare), MWCNT (\circ), activated carbon (\blacktriangle); c) Pyrolyzed PD (\blacktriangle), commercial D (\blacksquare), hydroxyl-functionalized D-OH (\circ); d) Carbocatalytic activity for the first (\blacksquare), second (\blacktriangle), third (\circ) and fourth use (∇) of the PD catalyst. Reaction conditions: Catalyst (50 mg L⁻¹), oxalic acid (50 mg L⁻¹), O₃ (140 mg/h), pH 3, 20 °C, O₃ to oxalic acid molar ratio 5.3.

The importance of an adequate HSAG functionalization at the edges by OH or COOH groups, preserving the sp² nature of the basal carbon atoms and the high work-function, was further evaluated by comparing the activity of non-selective HSAG functionalization with oxygen functional groups, in both edges and the basal planes, using a HNO₃ aqueous medium as oxidant. The carbocatalytic activity of the HSAG-

HNO₃ randomly functionalized with oxygen groups was clearly lower than that of HSAG-OH (Figure 5a). This activity order indicates the importance of the presence of sp² domains as active sites that should be well dispersed in water by selective edge functionalization.

To address the role of the sp² layer with a high work function due to presence of electron donor OH groups as active sites for O₃ activation other commercially available carbon allotropes such as graphite or CNTs were also tested. It was found that these materials also behave as active carbocatalysts in accordance with previous reports (Figure 5b).^{61, 62} The lower activity of graphite with respect to HSAG can be attributed to the lower specific surface area of the former and, therefore, the lower density of available sp² domains performing as active centers. The use of commercially available activated carbon as carbocatalysts resulted in lower activity with respect to carbon allotropes. A plausible explanation of the lower carbocatalytic activity of activated carbon with respect to the carbon allotropes would be the presence of sp³ domains on its amorphous carbon network. In fact, the activity of nanometric diamond constituted by sp³ carbons as carbocatalyst is negligible, a fact that is in agreement with our proposal of sp² domains as centers activating ozonation (Figure 5b). The use of a D solid functionalized with hydroxyl groups (D-OH) does not increase the activity of the D sample (Figure 5b). Notably, if nanometric D samples are submitted to pyrolysis at 900 °C for 2 h, as result of the surface graphitization of the D NPs, the resulting PD material is as active as HSAG-OH (Figure 4c). Attempts to reuse PD resulted in a decrease of the initial catalytic activity (Figure 4d). Interestingly, HSAG-OH and nanometric PD decompose rapidly O₃ (< 2 min) in the absence of oxalic acid at pH 3, while O₃ decomposition at pH 3 in the presence of commercial D NPs follows almost a coincident profile as that measured in the absence of any catalyst. All these findings

reinforce the role of high work-function sp^2 carbon layers as redox activator in ozonation, although it seems that they become partially oxidized, partially losing activity under reaction conditions.

According to this rationalization the role of phenolic groups in HSAG-OH would be to increase the electron density of the graphene layers that would act as electron donor versus ozone triggering the generation of reactive oxygen species (see below). Figure 6 illustrates the mechanistic proposal. Related with this rationalization Wang and co-workers have addressed by DFT the role of oxygens and edges as active sites donating electrons to peroxomonosulfate.⁶³ These $-OH$ groups can be considered as electron rich hydroquinone moieties.

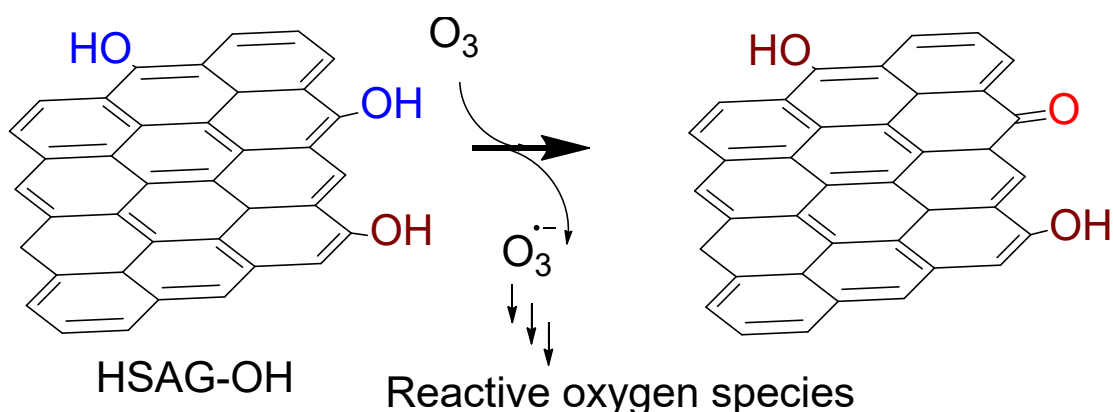


Figure 6. Proposed pathway for the oxidation of phenolic groups present in HSAG-OH to quinone-like moieties and one-electron reduction ozone and formation of reactive oxygen species.

Role of dispersibility

The previous proposal of sp^2 carbon domains with high work-function and phenol/quinone as redox pairs active sites for catalytic ozonation does not consider that the catalyst is constituted by graphite particles (HSAG-OH) that have low hydrophilicity and quickly sediment in a liquid due to the poor dispersability. To

address the role of other possible oxygenated functional groups increasing hydrophilicity and water dispersability, an analogous HSAG functionalized with carboxylic and hydroxyl groups in the graphene edges was prepared (HSAG-OH-COOH).⁴⁴ To make available the previously commented active sites and increase in hydrophilicity and dispersability should be beneficial. In this context, it is interesting to note that the activity of HSAG-OH-COOH is higher than that of HSAG-OH (Figure 4a). This result reinforces the idea that the activity of HSAG-based materials derives mainly from phenolic/quinone-like moieties and high work function of HSAG-OH layers derived from its unaltered sp^2 network combined with a high dispersibility of the graphite particles in water, due to the polar oxygen containing functional groups. The content of oxygenated functional groups was quantitatively evaluated (as described in the experimental part) using the Boehm titration method, which allows to determine groups such as carboxyls, lactones and phenolic. The total amounts of such functionalities were 0.75, 3.0 and 4.5 mmol/g for HSAG, HSAG-OH and HSAG-OH-COOH respectively. Water dispersions of HSAG-OH and HSAG-OH-COOH were prepared, at 1, 0.5, 0.1, 0.05, 0.01, 0.005 and 0.001 mg/mL as the nominal material concentration and UV-Vis absorption analysis was performed (Figures S9-S10). Details are reported in the supplementary material and in the experimental part. In particular, results from UV-Vis analysis of HSAG-OH and HSAG-OH-COOH suspensions in water, shown in Figures S10 and S11, reveal the larger stability of HSAG-OH-COOH dispersions.

Reactive oxygen species involved in the mechanism. In order to get some insight about the nature of reactive oxygen species formed during the catalytic ozonation in the presence of HSAG-OH catalyst, EPR measurements and selective radical quenching experiments were carried out. The use of DMPO as spin traps of reactive oxygen

species (ROS) derived from ozone in aqueous solution in the presence of HSAG-OH has allowed determining the presence of hydroperoxyl radicals (Figure 7a), while the use of TEMP reveals the formation of $^1\text{O}_2$ (Figure 7b). Selective quenching experiments using DMSO or *tert*-butanol do not inhibit the carbocatalytic oxalic degradation by ozone and, therefore, rule out the possible presence of hydroxyl radicals.²² These results are in agreement with those obtained by Shaobin and co-workers using rGO prepared by the Hummers method as carbocatalyst for ozone activation that have firmly ruled out by EPR measurements the possibility of hydroxyl radical generation.⁴² In contrast those studies have detected hydroperoxyl or $^1\text{O}_2$ species that were considered as responsible for the oxidation reaction.⁴² Those conclusions are coincident with those of the present study. In addition, in this work TOC measurements of the oxalic acid aqueous solution before and after the catalytic ozonation confirm the complete mineralization of the organic compound to CO_2 and H_2O .

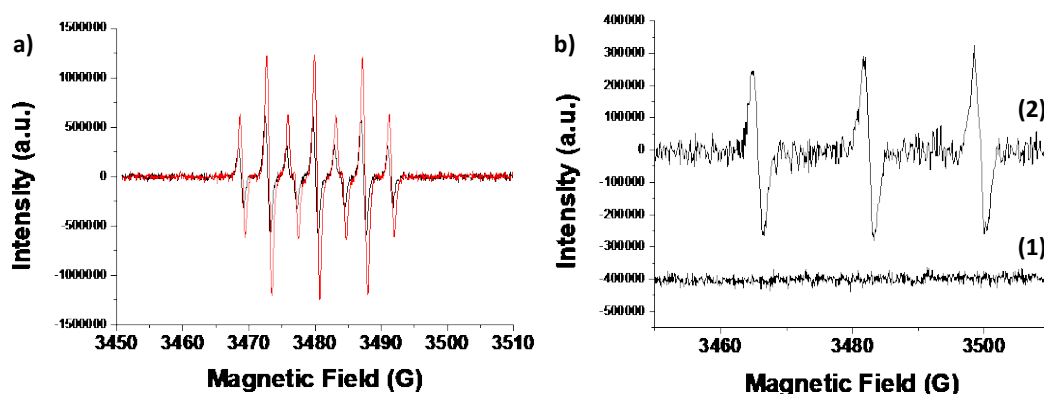


Figure 7. a) EPR spectra for ozonation in the presence of DMPO as trapping agent recorded in the absence (black line) or presence (red line) of HSAG-OH as catalyst. b) EPR spectra of O_3 in water in presence of TEMP as trapping agent recorded in the absence (1) and in the presence (2) of HSAG-OH as catalyst. Reaction conditions:

Catalyst (50 mg L^{-1}), O_3 (140 mg/h), trapping agent (1 g L^{-1}), pH 3, room temperature,
30 min reaction.

CONCLUSIONS

Using oxalic acid decomposition as probe reaction, the present manuscript has shown the catalytic activity for ozonation of a series of graphite and graphene materials at pH values in the range from 3 to 9. Higher pH values result in the spontaneous, fast, uncatalyzed decomposition of O₃. It was observed that optimal catalysts are those having sp² domains that can be well dispersed in water. This requires the presence of hydrophilic OH groups at peripheral positions without disturbing the sp² domains. Under the explored reaction conditions, it seems that graphene materials are prone to deactivate, due to auto-oxidation and that the presence of dopant element plays a detrimental effect in the catalytic activity. EPR measurements using spin trap agents and quenching experiments using selective inhibitors indicate that the reactive oxygen species generated in the process are mainly hydroperoxyl radicals and singlet oxygen. No evidence for the formation of hydroxyl radicals was obtained.

Considering the wide use of ozone for water disinfection, the present results open new opportunities for enhancement of ozone effect beyond disinfection for pollutant decomposition using transition metal-free catalysts based on carbon materials that can exhibit even and enhanced catalytic activity.

ASSOCIATED CONTENT

The following files are available free of charge. Characterization of the materials employed in the present work by XPS, TPD, Raman, ¹³C-NMR, UV-Vis analysis, HRTEM and kinetic of oxalic degradation by HSAG-OH.

AUTHOR INFORMATION

Corresponding Authors

* E-mail: hgarcia@qim.upv.es (H.G.)

* E-mail: sernaol@doctor.upv.es (S.N.)

* E-mail: maurizio.galimberti@polimi.it (M.G.)

* E-mail: vincenzina.barbera@polimi.it (V.A.)

Notes

The authors declare no competing financial interest.

ACKNOWLEDGMENT

Financial support by the Spanish Ministry of Science and Innovation (Severo Ochoa and RTI2018-098237-CO21) and Generalitat Valenciana (Prometeo 2017/083) is gratefully acknowledged. S.N. thanks financial support by the Fundación Ramón Areces (XVIII Concurso Nacional para la Adjudicación de Ayudas a la Investigación en Ciencias de la Vida y de la Materia, 2016), Ministerio de Ciencia, Innovación y Universidades RTI2018-099482-A-I00 project and Generalitat Valenciana grupos de investigación consolidables 2019 (ref: AICO/2019/214) project.

REFERENCES

1. Filonenko, G. A.; Van Putten, R.; Hensen, E. J. M.; Pidko, E. A., Catalytic (de)hydrogenation promoted by non-precious metals-Co, Fe and Mn: Recent advances in an emerging field. *Chem. Soc. Rev* **2018**, *47*, 1459-1483, DOI 10.1039/c7cs00334j.
2. Johansson Seechurn, C. C. C.; Kitching, M. O.; Colacot, T. J.; Snieckus, V., Palladium-catalyzed cross-coupling: A historical contextual perspective to the 2010 nobel prize. *Angew. Chem. Int. Ed.* **2012**, *51*, 5062-5085, DOI 10.1002/anie.201107017.
3. Leenders, S. H. A. M.; Gramage-Doria, R.; De Bruin, B., Reek, J.N.H. , Transition metal catalysis in confined spaces. *Chem. Soc. Rev.* **2015**, *44*, 433-448, DOI 10.1039/c4cs00192c
4. Magano, J.; Dunetz, J. R., Large-scale applications of transition metal-catalyzed couplings for the synthesis of pharmaceuticals. *Chem. Rev.* **2011**, *111*, 2177-2250, DOI 10.1021/cr100346g
5. Xia, Q.-H.; Ge, H.-Q.; Ye, C.-P.; Liu, Z.-M.; u, K.-X., Advances in homogeneous and heterogeneous catalytic asymmetric epoxidation. *Chem. Rev.* **2005**, *105*, 1603-1662, DOI 10.1021/cr0406458.
6. Brienza, M.; Katsoyiannis, I. A., Sulfate radical technologies as tertiary treatment for the removal of emerging contaminants from wastewater. *Sustainability* **2017**, *9*, 1604, DOI 10.3390/su9091604
7. Ikehata, K.; Jodeiri Naghashkar, N.; Gamal El-Din, M., Degradation of aqueous pharmaceuticals by ozonation and advanced oxidation processes: A review. *Ozone-Sci. Eng.* **2006**, *28*, 353-414, DOI 10.1080/01919510600985937.
8. Neyens, E., Baeyens, J., A review of classic Fenton's peroxidation as an advanced oxidation technique. *J. Hazard. Mater.* **2003**, *98*, 33-50, DOI 10.1016/S0304-3894(02)00282-0.
9. Pera-Titus, M.; García-Molina, V.; Baños, M. A.; Giménez, J.; Esplugas, S., Degradation of chlorophenols by means of advanced oxidation processes: A general review. *Appl. Catal. B-Environ* **2004**, *47*, 219-256, DOI 10.1016/j.apcatb.2003.09.010.
10. Pignatello, J. J.; Oliveros, E.; MacKay, A., Advanced oxidation processes for organic contaminant destruction based on the fenton reaction and related chemistry *Crit. Rev. Env. Sci. Tec.* **2006**, *36*, 1-84, DOI 10.1080/10643380500326564.
11. Klavarioti, M.; Mantzavinos, D.; Kassinos, D., Removal of residual pharmaceuticals from aqueous systems by advanced oxidation processes *Environ. Int.* **2009**, *35*, 402-417, DOI 10.1016/j.envint.2008.07.009.
12. Kasprzyk-Hordern, B.; Ziółek, M.; Nawrocki, J., Catalytic ozonation and methods of enhancing molecular ozone reactions in water treatment *Appl. Catal. B: Environ.* **2003**, *46*, 639-669, DOI 10.1016/S0926-3373(03)00326-6.
13. Muruganandham, M.; Suri, R. P. S.; Jafari, S.; Sillanpää, M.; Lee, G.-J.; Wu, J. J.; Swaminathan, M., Review article. Recent developments in homogeneous advanced oxidation processes for water and wastewater treatment. *Int. J. Photoenerg.* **2013**, *2014*, 821674, DOI 10.1155/2014/821674.
14. Beltrán, F. J.; Rivas, F. J.; Montero-de-Espinosa, R., Ozone-enhanced oxidation of oxalic acid in water with cobalt catalysts. 1. Homogeneous catalytic ozonation. *Ind. Eng. Chem. Res.* **2003**, *42*, 3210-3217, DOI 10.1021/ie0209982.
15. Hu, P.; Long, M., Cobalt-catalyzed sulfate radical-based advanced oxidation: A review on heterogeneous catalysts and applications. *Appl. Catal. B Environ.* **2016**, *181*, 103-117, DOI 10.1016/j.apcatb.2015.07.024.
16. Navalon, S.; Alvaro, M.; Garcia, H., Heterogeneous Fenton catalysts based on clays, silicas and zeolites. *Appl. Catal. B-Environ* **2010**, *99*, 1-26, DOI 10.1016/j.apcatb.2010.07.006

17. Navalon, S.; Dhakshinamoorthy, A.; Alvaro, M.; Garcia, H., Heterogeneous Fenton catalysts based on activated carbon and related materials. *ChemSusChem* **2011**, *4*, 1712-1730, DOI 10.1002/cssc.201100216.
18. Dhakshinamoorthy, A.; Navalon, S.; Alvaro, M.; Garcia, H., Metal nanoparticles as heterogeneous fenton catalyst. *ChemSusChem* **2012**, *5*, 46-64, DOI 10.1002/cssc.201100517.
19. Espinosa, J. C.; Catalá, C.; Navalón, S.; Ferrer, B.; Álvaro, M.; García, H., Iron oxide nanoparticles supported on diamond nanoparticles as efficient and stable catalyst for the visible light assisted Fenton reaction. *Appl Catal B: Environ.* **2018**, *226*, 242-251, DOI 10.1016/j.apcatb.2017.12.060.
20. Espinosa, J. C.; Manickam-Periyaraman, P.; Bernat-Quesada, F.; Sivanesan, S.; Álvaro, M.; García, H.; Navalón, S., Engineering of activated carbon surface to enhance the catalytic activity of supported cobalt oxide nanoparticles in peroxymonosulfate activation. *Appl Catal B: Environ.* **2019** *249*, 42-53, DOI 10.1016/j.apcatb.2019.02.043.
21. Nawrocki, J.; Kasprzyk-Hordern, B., The efficiency and mechanisms of catalytic ozonation. *Appl. Catal. B: Environ.* **2010**, *99*, 27-42, DOI 10.1016/j.apcatb.2010.06.033.
22. Ghuge, S. P.; Saroha, A. K., Catalytic ozonation for the treatment of synthetic and industrial effluents - Application of mesoporous materials: A review. *J. Environ. Manag.* **2018**, *21*, 83-102, DOI 10.1016/j.jenvman.2018.01.052.
23. Pines, D. S.; Reckhow, D. A., Effect of dissolved cobalt(II) on the ozonation of oxalic acid. *Environ. Sci. Technol.* **2002**, *36*, 4046-4051, DOI 10.1021/es011230w.
24. Wang, J.; Bai, Z., Fe-based catalysts for heterogeneous catalytic ozonation of emerging contaminants in water and wastewater. *Chem. Eng. J.* **2017**, *312*, 79-98, DOI 10.1016/j.cej.2016.11.118.
25. Titirici, M.-M.; White, R. J.; Brun, N.; Budarin, V. L.; Su, D. S.; del Monte, F.; Clark, J. H.; MacLachlan, M. J., Sustainable carbon materials. *Chem. Soc. Rev.* **2015**, *44*, 250-290, DOI 10.1039/C4CS00232F.
26. Duan, X.; Sun, H.; Wang, S., Metal-free carbocatalysis in advanced oxidation reaction. *Acc. Chem. Res.* **2018**, *513*, 678-687, DOI 10.1021/acs.accounts.7b00535.
27. Navalon, S.; Dhakshinamoorthy, A.; Alvaro, M.; Antonietti, M.; García, H., Active sites on graphene-based materials as metal-free catalysts. *Chem. Soc. Rev.* **2017**, *46*, 4501-4529, DOI 10.1039/C7CS00156H.
28. Navalon, S.; Dhakshinamoorthy, A.; Alvaro, M.; Garcia, H., Carbocatalysis by graphene-based materials. *Chem. Rev.* **2014**, *114*, 6179-6212, DOI 10.1021/cr4007347.
29. Álvarez, P. M.; García-Araya, J. F.; Beltrán, F. J.; Giráldez, I.; Jaramillo, J.; Gómez-Serrano, V., The influence of various factors on aqueous ozone decomposition by granular activated carbons and the development of a mechanistic approach. *Carbon* **2006**, *44*, 3102-3112, DOI 10.1016/j.carbon.2006.03.016.
30. Faria, P. C. C.; Órfão, J. J. M.; Pereira, M. F. R., Ozone decomposition in water catalysed by activated carbon: influence of chemical and textural properties. *Ind. Eng. Chem. Res.* **2006**, *45*, 2715-2721, DOI 10.1021/ie060056n.
31. Gonçalves, A. G.; Órfão, J. J. M.; Pereira, M. F. R., Catalytic ozonation of sulphamethoxazole in the presence of carbon materials: Catalytic performance and reaction pathways. *J. Hazard. Mater.* **2012**, *239-240*, 167-174, DOI 10.1016/j.jhazmat.2012.08.057.
32. Sánchez-Polo, M.; von Gunten, U.; Rivera-Utrilla, J., Efficiency of activated carbon to transform ozone into OH radicals: Influence of operational parameters. *Water Res.* **2005**, *39*, 3189-3198, DOI 10.1016/j.watres.2005.05.026.
33. Soares, O. S. G. P.; Faria, P. C. C.; Órfão, J. J. M.; Pereira, M. F. R., Ozonation of textile effluents and dye solutions in the presence of activated carbon under continuous operation. *Sep. Sci. Technol.* **2014**, *42*, 1477-1492, DOI 10.1080/01496390701290102.

34. Álvarez, P. M.; Beltrán, F. J.; Masa, F. J.; Pocostales, J. P., A comparison between catalytic ozonation and activated carbon adsorption/ozone-regeneration processes for wastewater treatment. *Appl Catal B: Environ.* **2009**, *92*, 393-400, DOI 10.1016/j.apcatb.2009.08.019.
35. Cao, H.; Xing, L.; Wu, G.; Xie, Y.; Shi, S.; Zhang, Y.; Minakata, D.; Crittendend, J. C., Promoting effect of nitration modification on activated carbon in the catalytic ozonation of oxalic acid. *Appl Catal B: Environ.* **2014**, *146*, 169-176, DOI 10.1016/j.apcatb.2013.05.006.
36. Faria, P. C. C.; Orfao, J. J. M.; Pereira, M. F. R., Catalytic ozonation of sulfonated aromatic compounds in the presence of activated carbon. *Appl Catal B: Environ.* **2008**, *83*, 150-159, DOI 10.1016/j.proenv.2013.04.066.
37. Sánchez-Polo, M.; Leyva-Ramos, R.; Rivera-Utrilla, J., Kinetics of 1,3,6-naphthalenetrisulphonic acid ozonation in presence of activated carbon. *Carbon* **2005**, *43*, 962-969, DOI 10.1016/j.carbon.2004.11.027.
38. Lin, Y.-C.; Chang, C.-L.; Lin, T.-S.; Bai, H.; Yan, M.-G.; Ko, F.-H.; Wu, C.-T.; Huang, C.-H., Application of physical vapor deposition process to modify activated carbon fibers for ozone reduction. *Korean J. Chem. Eng.* **2008**, *25*, 446-450, DOI 10.1007/s11814-008-0076-4.
39. Gonçalves, A. G.; Figueiredo, J. L.; Orfao, J. J. M.; Pereira, M. F. R., Influence of the surface chemistry of multi-walled carbon nanotubes on their activity as ozonation catalysts. *Carbon* **2010**, *48*, 4369-4381, DOI 10.1016/j.carbon.2010.07.051.
40. Geim, A. K.; Novoselov, K. S., The rise of graphene. *Natur. Mater.* **2007**, *6*, 183-191, DOI 10.1038/nmat1849.
41. Navalón, S.; Herance, J. R.; Álvaro, M.; García, H., General aspects in the use of graphenes in catalysis. *Mater. Horiz* **2018**, *5*, 363-378, DOI 10.1039/C8MH00066B.
42. Wang, Y.; Xie, Y.; Sun, H.; Xiao, J.; Cao, H.; Wang, S., Efficient catalytic ozonation over reduced graphene oxide for p-hydroxylbenzoic acid (PHBA) destruction: Active site and mechanism. *ACS Appl. Mater. Interfaces* **2016**, *8*, 9710-9720, DOI 10.1021/acsami.6b01175.
43. Pei, S.; Wei, Q.; Huang, K.; Cheng, H.-M.; Ren, W., Green synthesis of graphene oxide by seconds timescale water electrolytic oxidation. *Nat. Commun.* **2018**, *9*, 145, DOI 10.1038/s41467-017-02479-z.
44. Barbera, V.; Brambilla, L.; Porta, A.; Bongiovanni, R.; Vitale, A.; Torrisia, G.; Galimberti, M., Selective edge functionalization of graphene layers with oxygenated groups by means of Reimer–Tiemann and domino Reimer–Tiemann/Cannizzaro reactions. *J. Mater. Chem. A* **2018**, *6*, 7749-7761, DOI 10.1039/C8TA01606B.
45. Barbera, V.; Guerra, S.; Brambilla, L.; Maggio, M.; Serafini, A.; Conzatti, L.; Vitale, A.; Galimberti, M., Carbon papers and aerogels based on graphene layers and chitosan: Direct preparation from high surface area graphite. *Biomacromolecules* **2017**, *18*, 3978-3991, DOI 10.1021/acs.biomac.7b01026.
46. Barbera, V.; Porta, A.; Brambilla, L.; Guerra, S.; Serafini, A.; Valerio, A. M.; Vitale, A.; Galimberti, M., Polyhydroxylated few layer graphene for the preparation of flexible conductive carbon paper. *RSC Adv.* **2016**, *6*, 87767-87777, DOI 10.1039/C6RA19078B.
47. Galimberti, M.; Barbera, V.; Guerra, S.; Conzatti, L.; Castiglioni, C.; Brambilla, L.; Serafini, A., Biobased Janus molecule for the facile preparation of water solutions of few layer graphene sheets. *RSC Adv.* **2015**, *5*, 81142-81152, DOI 10.1039/C5RA11387C.
48. Espinosa, J. C.; Navalon, S.; Alvaro, M.; Dhakshinamoorthy, A.; Garcia, H., Reduction of C=C double bonds by hydrazine using active carbons as metal-free catalysts. *ACS Sustainable Chem. Eng.* **2018**, *6*, 5607-5614, DOI 10.1021/acssuschemeng.8b00638.
49. Vittore, A.; Acocella, M. R.; Guerra, G., Edge-oxidation of graphites by hydrogen peroxide. *Langmuir* **2019**, *35*, 2244-2250, DOI 10.1021/acs.langmuir.8b03489.

50. Duan, X.; Ao, Z.; Zhang, H.; Saunders, M.; Sun, H.; Shao, Z.; Wang, S., Nanodiamonds in sp²/sp³ configuration for radical to nonradical oxidation: Core-shell layer dependence. *Appl. Catal. B Environ.* **2018**, *222*, 176-181, DOI 10.1016/j.apcatb.2017.10.007.
51. Levanov, A. V.; Isaikina, O. Y.; Tyutyunnik, A. N.; Antipenko, E. E.; Lunin, V. V., Molar Absorption Coefficient of Ozone in Aqueous Solutions. *J. Anal. Chem.* **2016**, *6*, 549-553, DOI 10.1134/S1061934816060083.
52. Navalon, S.; Sempere, D.; Alvaro, M.; Garcia, H., Influence of hydrogen annealing on the photocatalytic activity of diamond-supported gold catalysts. *ACS Appl. Mater. Interfaces* **2013**, *5*, 7160-7169, DOI 10.1021/am401489n.
53. Petit, T.; Arnault, J.-C.; Girard, H. A.; Sennour, M.; Kang, T.-Y.; Cheng, C.-L.; Bergonzo, P., Oxygen hole doping of nanodiamond. *Nanoscale* **2012**, *4*, 6792-6799, DOI 10.1039/C2NR31655B.
54. Espinosa, J. C.; Navalón, S.; Primo, A.; Moral, M.; Fernández Sanz, J.; Álvaro, M.; García, H., Graphenes as efficient metal-free Fenton catalysts. *Chem. Eur. J.* **2015**, *21*, 11966-11971, DOI 10.1002/chem.201501533.
55. Sempere, D.; Navalon, S.; Danciková, M.; Alvaro, M.; Garcia, H., Influence of pretreatments on commercial diamond nanoparticles on the photocatalytic activity of supported gold nanoparticles under natural Sunlight irradiation. *Appl Catal B: Environ.* **2013**, *142-1743*, 259-267, DOI 10.1016/j.apcatb.2013.05.016.
56. Liu, J.-N.; Chen, Z.; Wu, Q.-Y.; Li, A.; Hu, H.-Y.; Yang, C., Ozone/graphene oxide catalytic oxidation: a novel method to degrade emerging organic contaminant N, N-diethyl-mtoluamide (DEET). *Sci. Rep.* **2016**, *6*, 31405, DOI 10.1038/srep31405.
57. Navalon, S.; Dhakshinamoorthy, A.; Alvaro, M.; Garcia, H., Metal nanoparticles supported on two-dimensional graphenes as heterogeneous catalysts. *Coord. Chem. Rev* **2016**, *312*, 99-148, DOI 10.1016/j.ccr.2015.12.005.
58. Qi, W.; Liu, W.; Zhang, B.; Gu, X.; Guo, X.; Su, D., Oxidative dehydrogenation on nanocarbon: Identification and quantification of active sites by chemical titration. *Angew.Chem.Int.Ed.* **2013**, *14224-14228*, DOI: 10.1002/anie.201306825.
59. Zhang, J.; Su, D. S.; Blume, R.; Schögl, R.; Wang, R.; Yang, X.; Gajovic, A., Surface chemistry and catalytic reactivity of a nanodiamond in the steam-free dehydrogenation of ethylbenzene. *Angew. Chem. Int. Ed.* **2010**, *49*, 8640-8644, DOI 10.1002/anie.201002869.
60. Espinosa, J. C.; Navalón, S.; Álvaro, M.; García, H., Reduced graphene oxide as a metal-free catalyst for the light-assisted Fenton-like reaction. *ChemCatChem* **2016**, *8*, 2642-2648, DOI 10.1002/cctc.201600364.
61. Sun, H.; Liu, S.; Zhou, G.; Ang, H. M.; Tade, M. O.; Wang, S., Reduced Graphene Oxide for Catalytic Oxidation of Aqueous Organic. *ACS Appl. Mater. Interfaces* **2012**, *4*, 5466-5471, DOI 10.1021/am301372d.
62. Zhang, S.; Quan, X.; Zheng, J.-F.; Wang, D., Probing the interphase "HO[rad] zone" originated by carbon nanotube during catalytic ozonation. *Water. Res.* **2017**, *122*, 86-95, DOI 10.1016/j.watres.2017.05.063.
63. Duan, X.; Sun, H.; Ao, Z.; Zhou, L.; Wang, G.; Wang, S., Unveiling the active sites of graphene-catalyzed peroxy monosulfate activation. *Carbon* **2016**, *107*, 371-378, DOI 10.1016/j.carbon.2016.06.016.

For Table of Contents Use Only.

